Carbohydrate Research, 61 (1978) 27–40

THE DOUBLE-HELICAL MOLECULAR STRUCTURE OF CRYSTALLINE A-AMYLOSE*†

HSIEN-CHIH HAROLD WU AND ANATOLE SARKO‡

Department of Chemistry, SUNY College of Environmental Science and Forestry, Syracuse, New York 13210 (U.S.A.)

(Received June 6th, 1977; accepted for publication in revised form, November 2nd, 1977)

ABSTRACT

As was found with B-amylose (see preceding paper), the crystal structure of A-amylose is apparently based on parallel-stranded, right-handed double helices. The helices pack in antiparallel fashion into an orthorhombic unit-cell (a = 11.90, b = 17.70, c (fiber repeat) = 10.52 Å), which results in nearly hexagonal close-packing. The steric disposition of O-6 is either all *gt* or may be a mixture of *gt* and *tg*. The unit cell of A-amylose contains only about a quarter of the water molecules located in the unit cell of B-amylose. Aside from the differences in the amount of water, the A and B structures differ only in that the former has a denser packing-structure, whereas the latter is more open. The similarities in packing suggest that interconversions of A and B are possible. Experimentally, partial conversion of B into A has been observed.

INTRODUCTION

Of the two major starch polymorphs — A and B — very little structural information is available on type A. The granules of A-starch appear to be as crystalline as B-starch, but the diffraction diagrams obtained from the two starches are considerably different. We have shown that pure amylose can crystallize in both A and B polymorphic forms, yielding X-ray diagrams that are identical with the corresponding diagrams of A- and B-starches[1–3]. The amylose polymorphs are much more suitable than starch for structural analysis because they can be oriented to give fiber diagrams of good quality. In a previous communication, we reported a unit cell for A-amylose and presented evidence that its crystal structure was likely to be double helical[1]. We are now able to report a successful crystal-structure determination of A-amylose that clearly points to a double-helical structure. This work was conducted in parallel with that on B-amylose reported in the preceding paper[2]. The two structures are

*Dedicated to Professor Dexter French on the occasion of his 60th birthday.
†Part IX in the series "Packing Analysis of Carbohydrates and Polysaccharides".
‡To whom correspondence should be addressed.

nearly identical in molecular conformation, but they differ considerably with respect to the packing of the helices in the crystal structure. This raises interesting questions regarding the biosynthesis of the two types of starch.

EXPERIMENTAL

The preparation of a crystalline, fiber specimen of A-amylose and its X-ray diffraction diagram have been previously reported by us[1]. It is interesting to compare the conditions necessary for the preparation of either A- or B-amylose from alkali amylose, which is the starting point for both polymorphs. In order to obtain B-amylose, the alkali amylose is exposed to high relative humidity (r.h.) at room temperature, followed by heating in water[2]. On the other hand, A-amylose is obtained when the alkali amylose is exposed to the same high r.h., but at temperatures of 85° or higher. Once either pure polymorph has been obtained, neither is completely convertible into the other, whereas, under certain conditions, B-amylose may be converted into a mixture of A- and B-amyloses.

The X-ray diffraction intensities for A-amylose were measured and converted into relative structure-amplitudes as described for B-amylose[2]. In order to make the corrected intensities approach zero at diffraction angles where they appeared to vanish in the X-ray diffraction diagram, the final corrected intensities were multiplied by an artificial temperature-factor[4] $e^{-a^2s^2}$, where $a = 2.0$ and $s = \tan 2\theta$.

RESULTS OF STRUCTURE ANALYSIS

Unit cell. — As previously reported[1], the unit cell of A-amylose is orthorhombic, with $a = 11.90 \pm 0.06$ Å, $b = 17.70 \pm 0.10$ Å and c (fiber repeat) $= 10.52 \pm 0.10$ Å. The fiber repeat is slightly (and probably insignificantly) different from that of B-amylose, for which $c = 10.40$ Å (ref. 2). Neither the $P2_1$ nor the $P2_12_12_1$ space group is applicable. A third-order meridional is clearly visible in diffractograms of tilted fibers. The measured density of the fiber is 1.51 g/cm^3, which is in agreement with 12 D-glucose residues per cell and up to 8 water molecules ($\rho_{calc} = 1.56$ g/cm^3). Elemental analysis of a fiber stored at 80% r.h. indicated 10.5 ± 1.5 water molecules per cell. These data, as well as Patterson and Fourier projections along the fiber axis, indicate that the unit cell is traversed by two helices, one at the corner and the other at the center of the cell. Each such helix could be either a single, six-fold helix repeating in $c = 10.52$ Å or a double-stranded helix having six residues per turn, each strand repeating in 21.04 Å. In order for the single, six-fold helix to exhibit a third-order meridional, it would have to be based on a repeating unit composed of two structurally dissimilar D-glucose residues. As previously stated[1], the observed fiber pattern of A-amylose accounts for all of the reflections seen in powder patterns of A-starch.

Stereochemical-model analysis. — The probability of the foregoing two classes of helices was tested with a combined conformation-packing refinement as described

TABLE I

PACKING OF PARALLEL-STRANDED DOUBLE HELICES AND SINGLE, SIX-FOLD HELICES HAVING VB = 4.25 Å

Helix type	*Chirality*	*O-6*[a] *(deg.)*	*Bridge angle (deg.)*	*P.E.*[b] *(pack./ conf.)*	*Helix positions*[c]			*Hydrogen bonds and length, Å*[a]		*Short packing contacts*
					Helix 1 rotation (deg.)	*Helix 2 rotation (deg.)*	*Helix 2 translation (Å)*			
Double, antiparallel packed	Right-handed	*gt* (51)	106	16/27	−3.9	1.4	1.13	$O\text{-}2_2\text{–}O\text{-}2_9$ $O\text{-}2_3\text{–}O\text{-}2_8$ $O\text{-}6_5\text{–}O\text{-}6_{10}$ $O\text{-}6_4\text{–}O\text{-}6_{11}$	2.95 2.85 2.68 2.77	None
Double antiparallel packed	Left-handed	*gg* (−77)	103	30/26	−9.7	10.9	−1.65	$O\text{-}3_4\text{–}O\text{-}3_{11}$ $O\text{-}3_5\text{–}O\text{-}3_{10}$	2.88 2.83	None
Double, parallel packed	Right-handed	*tg* (151)	106	32/28	1.5	−4.6	0.83	$O\text{-}2_2\text{–}O\text{-}6_7$ $O\text{-}2_2\text{–}O\text{-}2_{11}$ $O\text{-}6_2\text{–}O\text{-}6_{11}$	2.97 2.58 2.56	None
Double, parallel packed	Left-handed	*gg* (−76)	104	32/26	−10.9	−60.0	2.59	$O\text{-}2_4\text{–}O\text{-}6_8$ $O\text{-}6_4\text{–}O\text{-}2_{11}$	2.98 2.73	None
Single, antiparallel packed[e]	Right-handed	—	118	83/17[e]	16.9	−19.4	−0.22	None		8 contacts[e]
Single, antiparallel packed[e]	Left-handed	—	117	68/12[e]	−34.6	34.8	1.39	None		9 contacts[e]
Single, parallel packed[e]	Right-handed	—	119	74/13[e]	13.5	13.5	0.0	None		8 contacts[e]
Single, parallel packed[e]	Left-handed	—	118	106/12[e]	3.8	3.5	−0.01	None		8 contacts[e]

[a]O-6 is at 0° when the bond sequence O-5–C-5–C-6–O-6 is *cis*. Rotation of C-6–O-6 is positive–clockwise looking from C-5 to C-6, and pure *gt* = 60°, *tg* = 180°, *gg* = −60°. [b]P.E. = packing energy, from the nonbonded term of Eq. *1* of ref. 2. The first number indicates inter-strand and inter-helix packing energy, while the second indicates intra-chain, or conformational energy. For reasonable models, this packing energy should not exceed the high 30's. [c]Helix 1 is at the corner and helix 2 is in the center of the unit cell. The 0° rotational position for helix 1 is with O-4 at $x = 0, -y$; for helix 2 with $O\text{-}4_7$ at $x = a/2, y = b/2 - y$ ($O\text{-}4_1$). Positive rotation is clockwise looking down the *c* axis. Translation of helix 2 is relative to helix 1 along *c*. [d]Subscripts indicate residue numbers: 1–3 are in chain 1 of helix 1, 4–6 are in chain 2 of helix 1, 7–9 are in chain 1 of helix 2, and 10–12 are in chain 2 of helix 2. [e]*O-6 contacts not included.*

TABLE II

PACKING OF HELICES HAVING DIFFERENT VIRTUAL BOND-LENGTHS

Helix type	*Chirality*	*VB[a] (Å)*	*Bridge angle (deg.)*	*P.E.[b] (pack./ conf.)*	*Short packing contacts*
Double, antiparallel packed, O-6 *gt*	Right-handed	4.25	106	16/27	None
		4.45	116	49/21	
Double, parallel packed, O-6 *gt*	Right-handed	4.25	106	35/27	None
		4.45	114	66/23	
Single, antiparallel packed[c]	Right-handed	4.00	110	81/19[c]	10 contacts[c]
		4.25	118	83/17[c]	8 contacts[c]
Single, antiparallel packed[c]	Left-handed	4.00	106	56/18[c]	2 contacts[c]
		4.25	117	68/12[c]	9 contacts[c]
Single, parallel packed[c]	Right-handed	4.00	110	50/17[c]	8 contacts[c]
		4.25	119	74/13[c]	8 contacts[c]
Single, parallel packed[c]	Left-handed	4.00	109	75/16[c]	7 contacts[c]
		4.25	118	106/12[c]	7 contacts[c]

[a]Virtual bond-length. [b]See footnote *b* in Table I. [c]O-6 contacts not included.

for B-amylose[2]. Included in the two classes were two single helices: 6_1 (right-handed) and 6_5 (left-handed), forgetting for the moment the requirement for a disaccharide repeating-unit; and two double-helices: parallel-stranded, parallel-packed (that is, both corner and center helices of the same packing polarity), and parallel-stranded, antiparallel-packed. The antiparallel-stranded double helices were ruled out on conformational grounds, as they had been for B-amylose[2]. The double helices were tested both in left- and right-handed conformations.

The results of this analysis are illustrated in Tables I and II, in terms of packing and conformational energies as defined in the preceding paper describing B-amylose[2]. In the interest of brevity, only representative models are shown in Table I for a fixed virtual bond-length of 4.25 Å, whereas Table II shows a comparison in which virtual bond-lengths are varied.

Of the single helices, both the 6_1 and the 6_5 conformation constructed with a virtual bond-length of 4.25 Å had too many serious short contacts to be considered as probable models for A-amylose. The 4.25-Å virtual bond-length is one of the shorter D-glucose residues found in single-crystal analyses of carbohydrates, and results in a helix of relatively narrow diameter. When the same analysis was repeated with a 4.0-Å virtual bond residue — one that results in an even narrower helix, but one that has not been found in carbohydrates — no improvement was seen in the packing (Table II). On this basis, six-fold, single helices were eliminated from further consideration.

As had been the case with B-amylose, parallel-stranded double helices of either handedness were conformationally probable for various residue lengths, although with different bridge angles. For example, for a virtual bond of 4.25 Å in length, the

bridge angle was 105 ± 1°, whereas for the 4.45-Å virtual bond, it was 116 ± 1° and for the 4.60-Å bond it was 118 ± 1°. However, packing difficulties observed with the longer virtual bonds restricted the double-helical conformations to models having VB = 4.25 Å and a consequent, low bridge-angle of 105–106°. For such double helices, both parallel and antiparallel packing were possible, regardless of helix chirality, and for all three primary rotational positions of O-6. There were no inter-strand or inter-helical short contacts in any of these double helices, and all formed several inter-helical hydrogen bonds (compare Table I).

In addition to the double and six-fold single helices, three-fold helices were tested in several four-chain per cell packing-modes. The latter are shown in Fig. 1. This was done primarily because of the presence of the *003* meridional reflection and in spite of disagreement with the Patterson projection and despite the fact that conformationally, such chains are improbable[1]. As expected, none of these packing modes were possible. Thus, only the double helices remained as viable models. The results obtained with the latter duplicate those obtained for B-amylose, both with respect to residue length as well as helix chirality and polarity of packing. However, as was the case with B-amylose, the most probable double-helical model could not be picked solely on the basis of stereochemical refinement; therefore, all of the models were further refined against the X-ray intensities.

X-Ray refinement. — Because of the large number of models that had to be

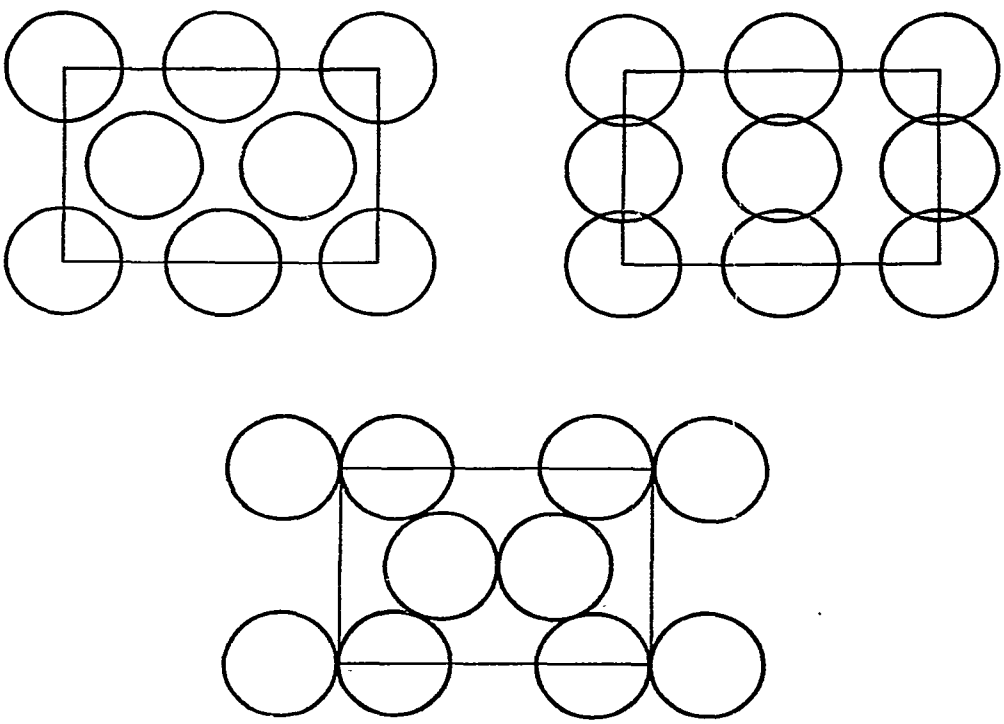

Fig. 1. Three possible packing-modes of four three-fold helices tested in this work.

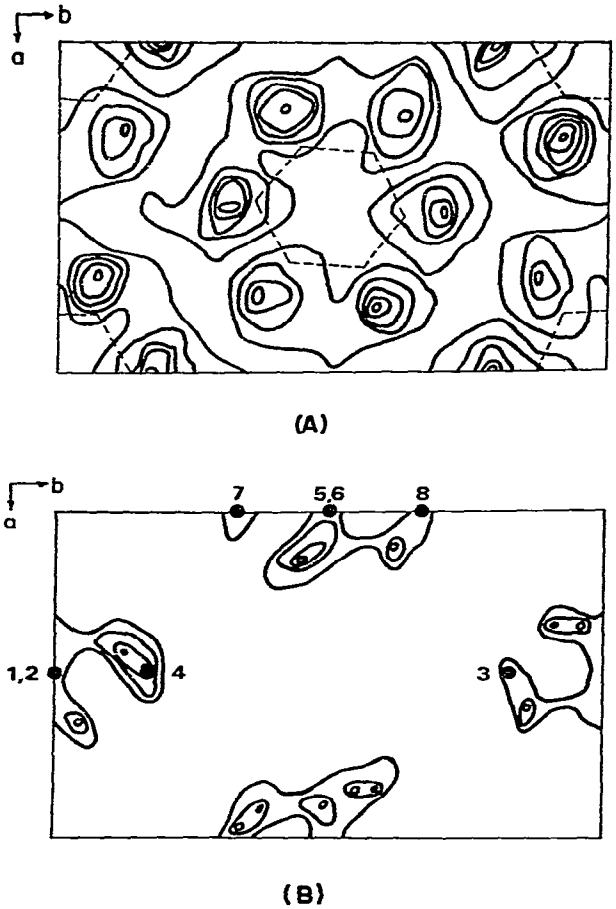

Fig. 2. Fourier projection (A) and difference-Fourier (B) calculated with observed, equatorial structure-amplitudes. The phasing model is a double-stranded, right-handed helix. The virtual bonds are indicated by dashed lines. The numbered positions in the difference-Fourier projection indicate locations into which water molecules were subsequently placed.

tested against diffraction intensities and the necessity, at the same time, to locate water molecules, preliminary X-ray refinement was made in projection, using equatorial intensities only. A sufficient number of equatorial reflections and the reliability of their intensities made this procedure feasible.

Two-dimensional refinement and location of water. The apparent positions of water molecules were much less clear-cut for A-amylose than they were for B-amylose. However, both Fourier and difference-Fourier projections calculated with observed structure-amplitudes and phased with different double-helical models all indicated the regions shown in Fig. 2 as likely to contain water. From packing considerations, both regions also appeared to contain sufficient void space to accommodate up to four water molecules each.

The number of water molecules, as well as their approximate x–y coordinates, were then determined by a systematic testing of each model. In this testing, different numbers of water molecules were inserted in the indicated space and systematically moved in the a–b plane, while at the same time rotating both helices about their axes within a 60° sector. The chain conformations were held fixed. Included in this testing were conformations having longer virtual bonds, even though they had been eliminated on stereochemical grounds. The crystallographic reliability index,

$$R = \frac{\sum| \, |F_c| - |F_o| \, |}{\sum |F_o|},$$

(where F_c and F_o are the equatorial calculated and observed structure amplitudes, respectively), was the sole criterion for evaluating each combination.

Best results were obtained with eight water molecules per cell, although for some models, six water molecules were almost as good. The results are shown in Table III, in detail for the best model and only partially for other models. For comparison, the R-values for cells containing no water are also shown. All other combinations of water molecules gave much higher R-values and were not considered

TABLE III

TWO-DIMENSIONAL R-VALUES IN SYSTEMATIC TESTING OF DOUBLE-HELICAL MODELS HAVING VARIOUS WATER ARRANGEMENTS

Helix	*VB*[a] *(Å)*	*No. of H_2O in unit cell*	*Arrangement of H_2O*[b] *(Å)*	R-*Value*
Right-handed, antiparallel-packed, O-6 *gt*	4.25	8	0	0.31
			0, ±1.0	0.29
			0, ±2.0	0.25
			0, ±3.0	0.21
			0, ±4.0	0.31
		6	0, ±3.0	0.24
		No water		0.37
	4.45	8	0, ±3.0	0.38
		No water		0.44
	4.60	8	0, ±3.0	0.45
		No water		0.47
Right-handed, antiparallel-packed, O-6 *tg*	4.25	8	0, ±3.0	0.28
		No water		0.44
Right-handed, parallel-packed, O-6 *gt*	4.25	8	0, ±3.0	0.24
		No water		0.44
Left-handed, antiparallel-packed, O-6 *tg*	4.25	8	0, ±2.5	0.31
		No water		0.36
Left-handed, parallel-packed, O-6 *gg*	4.25	8	0, ±3.0	0.29
		No water		0.36

[a]Virtual bond-length. [b]Positions of H_2O are relative to $a/2$ and $b/2$. For example, 0, ±3.0 indicates that water molecules 1 and 2 are at $a/2$, 0; 3 and 4 are at $a/2$ ±3.0, 5 and 6 are at 0, $b/2$; and 7 and 8 are at 0, $b/2$ ±3.0 (compare Fig. 2).

further. The best model in each category was further subjected to two-dimensional refinement, with positions of water molecules as variables. Two best models remained, both right-handed double helices in antiparallel packing with VB = 4.25 Å. The two models differed only in rotation about O-6: the first and better of the two had O-6 *gt* whereas the second had O-6 *tg*. These two models were then subjected to three-dimensional refinement.

Final structure refinement. The surviving two models were refined against three-dimensional X-ray data in two stages. In the first stage, the translation of the center helix of the unit cell along its axis and the coordinates of the water molecules were obtained by systematic testing, using the three-dimensional *R*-value and stereochemical packing-energies as criteria for the goodness of the model. As expected, the optimal helix-translation thus found did not coincide with that found in earlier stereochemical refinement. The reasons for the disagreement stem from not having water molecules included in the stereochemical refinement and the fact that there are several packing minima along the helix axes.

In the second stage of refinement, all likely models found in the first stage were subjected to a complete, combined X-ray and stereochemical refinement, where the function[5]

$$\phi = fR + (1 - f)\, Y \qquad (1)$$

was minimized. (In this function, R is the three-dimensional R-factor, Y is the packing-conformation energy, and f is the fractional weight of the R-factor in the linear combination. In this instance, a value of $f = 0.9$ was used, which resulted in approximately equal weight for R and Y). The necessity for using the combined refinement-function arose because, in the absence of any stereochemical constraints, the R-factor refinement tended to move the water molecules into unreasonable packing-positions.

In this refinement, the variables were initially rotation and translation of the helices, rotation of the sugar residue about the virtual bond, rotameric angle for O-6, and the x,y,z coordinates of the water molecules. For the latter, the movement of water molecules 3 and 4 were coupled together, as if a two-fold rotation axis were present at $1/2a$, $0b$. Water molecules 7 and 8 were similarly coupled with respect to an imaginary diad at $0a$, $1/2b$. The double parallel-stranded helical structure, having the two strands exactly 180° out of phase, makes such a coupling of water molecules almost mandatory. In the later refinements, bond and conformational angles were also allowed to vary, but these additional variables did not significantly improve the results.

Both of the structures — parallel-stranded double helices in antiparallel packing with VB = 4.25 Å, but differing only in rotations about O-6 — refined to nearly identical R-values: 0.37 for the O-6 *gt* model and 0.36 for the O-6 *tg* model. The characteristics of both models are shown in Table IV, and their calculated structure-amplitudes are given in Table V. Their helix rotations and translation had very small ranges, about 1° for rotation and 0.2 Å for translation, as was found in B-amylose.

TABLE IV

CHARACTERISTICS OF THE FINAL TWO DOUBLE-HELICAL MODELS

Helix	*O-6*[a] *(deg.)*	*Bridge angle (deg.)*	*VB*[b] *(Å)*	*Helix positions*[c]			*Hydrogen bonds and lengths (Å)*[d]	*Short packing contacts*[d]
				Helix 1 rotation (deg.)	*Helix 2 rotation (deg.)*	*Helix 2 translation (Å)*		
Right-handed antiparallel packed	*gt* (61)	105	4.25	−10.0	0.0	6.4	$O\text{-}3_1\text{–}O\text{-}6_2$ 2.78 $O\text{-}5_6\text{–}O\text{-}6_{11}$ 2.77 (27 additional hydrogen bonds to water molecules)	$H\text{-}6_8\text{–}O\text{-}2_9$ 1.90 $O\text{-}2_2\text{–}H\text{-}2_7$ 2.09
Right-handed, antiparallel packed	*tg* (144)	106	4.25	−20.0	0.0	5.2	$O\text{-}3_2\text{–}O\text{-}6_4$ 2.66 $O\text{-}2_2\text{–}O\text{-}3_7$ 2.92 $O\text{-}5_1\text{–}O\text{-}6_7$ 2.90 $O\text{-}2_1\text{–}O\text{-}2_4$ 2.79 $O\text{-}2_6\text{–}O\text{-}2_8$ 2.59 (26 additional hydrogen bonds to water molecules)	$O\text{-}2_6\text{–}H\text{-}4_9$ 2.12 $O\text{-}2_3\text{–}H\text{-}4_{12}$ 2.12

[a]See footnote *a* in Table I. [b]Virtual bond-length. [c]See footnote *c* in Table I. [d]See footnote *d* in Table I.

TABLE V

OBSERVED AND CALCULATED STRUCTURE AMPLITUDES FOR THE BEST TWO MODELS OF A-AMYLOSE

hkl	$F_{obs.}$	$F_{calc.}$		hkl	$F_{obs.}$	$F_{calc.}$	
		O-6 gt	*O-6 tg*			*O-6 gt*	*O-6 tg*
010	4	0	0	311	280	46	103
100	4	0	1	321, 241			
110	10	1	31	051, 331, 151	191	185	148
020	57	48	49	251, 401			
120	5	1	0	341, 061, 411	224	344	368
200, 030, 210	282	238	285	161, 421	192	220	223
130	307	318	407	012	33	17	21
220	385	359	331	102, 112	46	214	114
040	243	181	161	022	23	151	70
230	19	14	26	122	24	19	23
140	18	8	9	202, 032			
300	18	9	31	132, 212, 222	360	223	325
310	259	142	80	042	126	137	106
320, 240, 050	207	230	169	232, 142			
150, 330	168	294	211	312, 302	265	289	257
250, 400				322, 242			
340, 060, 410	283	213	176	052, 152, 332	249	295	314
160, 420	168	111	143	013	21	6	174
430, 260, 350	257	135	199	103	22	69	83
070, 170, 440	142	149	118	113	24	110	87
011	55	60	33	023, 123	59	94	124
101, 111	97	164	86	203, 213, 033	164	108	143
021	20	97	47	133, 223			
121	233	241	318	043, 233	229	296	258
201, 031				143, 303, 313	242	219	293
211, 131	402	376	485	323, 243, 053	107	254	214
221	109	177	77				
041, 231							
141, 301	396	171	175				

With the exception of the O-6 position, both models are similar in their gross features and neither one can be selected as the most probable structure. Both are able to form numerous hydrogen bonds and neither model contains bad short-contacts. In view of the similarity of the two models and the fact that both show different discrepancies between calculated and observed structure-factors (compare Table V), it is conceivable that the true structure is a mixture of both. For example, the *R*-value for a 50:50 mixture is 0.34, which is not in disagreement with this argument. Otherwise, on the basis of similarity to the structure of B-amylose, the model having O-6 *gt* would be the more likely of the two. The atomic coordinates of this model are shown in Table VI and its unit-cell structure is shown in a stereo view in Fig. 3. The bond and conformation angles of the D-glucose residue in this model are mostly within one standard deviation of the corresponding average values[6]. It should be noted that all attempts

TABLE VI

CARTESIAN ATOMIC COORDINATES OF ONE RESIDUE OF EACH CHAIN OF THE MODEL HAVING O-6 *gt*

Atom	x (Å)	y (Å)	z (Å)	*Atom*	x (Å)	y (Å)	z (Å)
1. Corner helix, chain 1				*3. Center helix, chain 1*			
C-1	3.017	−1.970	3.127	C-1	3.321	6.386	3.273
C-2	3.649	−1.761	1.752	C-2	2.662	6.483	4.648
C-3	2.543	−1.621	0.718	C-3	3.727	6.812	5.682
C-4	1.523	−2.742	0.816	C-4	4.926	5.885	5.584
C-5	1.029	−2.948	2.253	C-5	5.448	5.768	4.147
C-6	0.214	−4.213	2.450	C-6	6.470	4.664	3.950
O-1	2.258	−0.822	3.506	O-1	3.869	7.649	2.894
O-2	4.475	−0.614	1.739	O-2	1.650	7.469	4.661
O-3	3.138	−1.645	−0.580	O-3	3.145	6.685	6.980
O-4	0.417	−2.367	0.0	O-4	5.950	6.447	6.400
O-5	2.163	−3.096	3.124	O-5	4.357	5.426	3.276
O-6	−0.223	−4.352	3.798	O-6	6.925	4.603	2.602
H-1	3.779	−2.122	3.833	H-1	2.597	6.104	2.567
H-2	4.232	−2.601	1.515	H-2	2.234	5.554	4.885
H-3	2.057	−0.701	0.856	H-3	4.046	7.803	5.544
H-4	1.942	−3.635	0.454	H-4	4.668	4.933	5.946
H-5	0.463	−2.116	2.553	H-5	5.861	6.685	3.847
H-6a	0.792	−5.048	2.182	H-6a	6.046	3.741	4.219
H-6b	−0.628	−4.171	1.826	H-6b	7.293	4.851	4.574
2. Chain 2				*4. Chain 2*			
C-1	−3.017	1.970	3.127	C-1	8.579	11.314	3.273
C-2	−3.649	1.761	1.752	C-2	9.238	11.217	4.648
C-3	−2.543	1.621	0.718	C-3	8.173	10.888	5.682
C-4	−1.523	2.742	0.816	C-4	6.974	11.815	5.584
C-5	−1.029	2.948	2.253	C-5	6.452	11.932	4.147
C-6	−0.214	4.213	2.450	C-6	5.430	13.036	3.950
O-1	−2.258	0.822	3.506	O-1	8.031	10.052	2.894
O-2	−4.475	0.614	1.739	O-2	10.250	10.231	4.661
O-3	−3.138	1.645	−0.580	O-3	8.755	11.015	6.980
O-4	−0.417	2.367	0.0	O-4	5.950	11.253	6.400
O-5	−2.163	3.096	3.124	O-5	7.543	12.274	3.276
O-6	0.223	4.352	3.798	O-6	4.975	13.097	2.602
H-1	−3.779	2.122	3.833	H-1	9.303	11.596	2.567
H-2	−4.232	2.601	1.515	H-2	9.666	12.146	4.885
H-3	−2.057	0.701	0.856	H-3	7.854	9.897	5.544
H-4	−1.942	3.635	0.454	H-4	7.232	12.767	5.946
H-5	−0.463	2.116	2.553	H-5	6.039	11.015	3.847
H-6a	−0.792	5.048	2.181	H-6a	5.854	13.959	4.219
H-6b	0.628	4.171	1.826	H-6b	4.607	12.849	4.574
				5. Water molecules			
				W-1	5.950	0.0	−0.500
				W-2	5.950	0.0	−5.500
				W-3	6.384	−2.462	2.500
				W-4	5.516	2.462	2.500
				W-5	0.0	8.850	−1.500
				W-6	0.0	8.850	1.00
				W-7	0.370	6.377	4.00
				W-8	0.370	11.323	−4.00

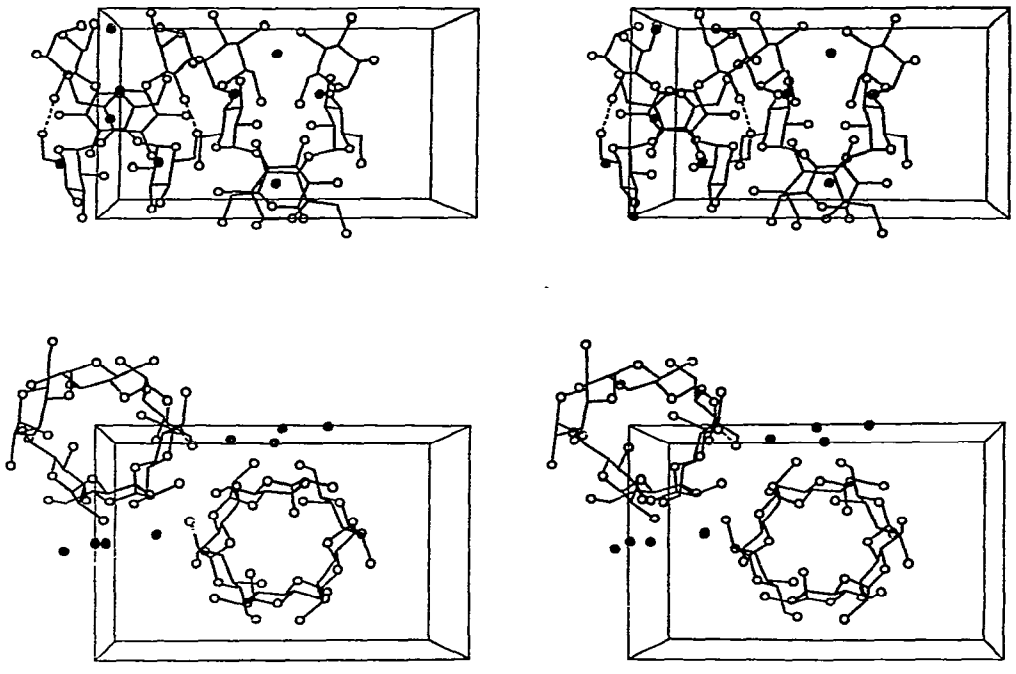

Fig. 3. The unit cell and crystal structure of A-amylose in stereo views. Top: side view, bottom: view down the helix axis. Water molecules are indicated in the lower view by dots. Hydrogen atoms are not shown. Hydrogen bonds are indicated by dashed lines.

to force the bridge angle of the VB = 4.25 Å model to values larger than 105–106° resulted in much poorer *R*-values.

DISCUSSION

A comparison of the structures of A- and B-amylose reveals considerable similarities. To some extent, this is expected because the fiber repeats of both structures and the lateral distances between helices are virtually identical. The packing of the helices also shows some similarity — compare Fig. 4 — because the A-structure may be imagined to be built up from the B-structure simply by inserting another helix in the latter in place of the water column. Consequently, such features as the polarity of packing, the rotational positions of the helices, and the conformation angle of the O-6 atoms can be expected to be reasonably similar. The translational positions of helices are different, but this is not surprising in view of the different water environments of the helices in the two structures.

The bridge angle at the glycosidic oxygen atom also turned out to be identical at about 105° in both structures. This finding, arrived at independently in two structures, argues for the reliability of this unexpectedly small bridge-angle and against its being an artifact of refinement.

Further comparing the reliability of the A- and B-structures, the *R*-value for

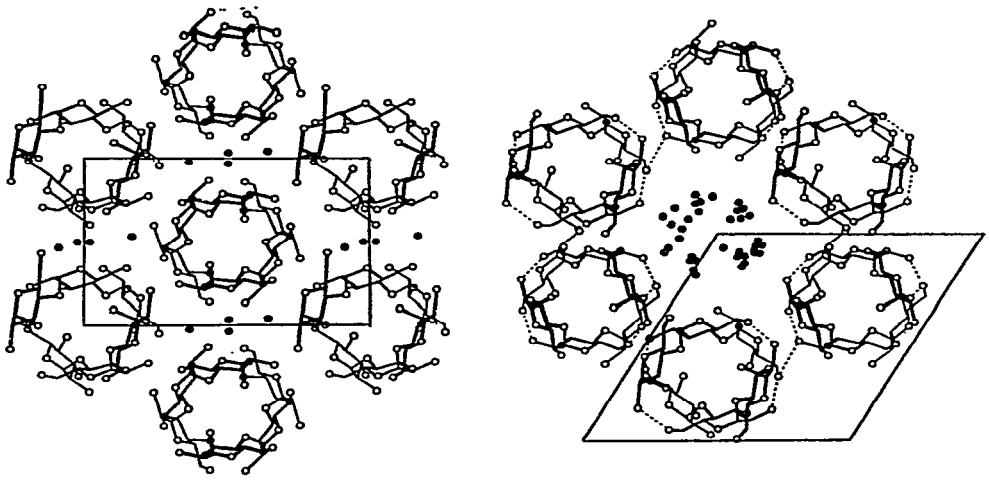

Fig. 4. Comparison of unit cells and helix packing in A- and B-amylose.

B-amylose was considerably better than that for A-amylose. To some extent this is deceptive, because in B-amylose the water positions were stereochemically not constrained, whereas in A-amylose they were. The *R*-value for the latter can be improved by letting the water molecules refine their positions in an unrestricted manner, particularly in the *z*-direction, but the wisdom of this is questionable. It is clear that the number and arrangement of water molecules found here represents a refinement minimum, but whether it is the best or only minimum is not known. Many more X-ray data would be needed to answer this question. It is also true, however, that the higher-layer reflections in the A-amylose diagram are more arced than those of the B-amylose, and therefore, their intensities are somewhat less reliable.

In B-amylose, the diameter of the channel occupied by water is more than sufficiently large to accommodate atoms of iodine (the atomic diameter of iodine in the gas phase is $\sim$ 2.7 Å). This could provide the mechanism whereby iodine is absorbed by granular starch to give the characteristic blue color. In A-amylose, however, the channel occupied by water is much smaller and it is not certain whether a sufficient number of iodine molecules could squeeze into it to produce the intense blue normally seen in starch–iodine mixtures. On the other hand, we have not been able to demonstrate iodine uptake by fibrous specimens of either B- or A-amylose. Such specimens are normally much more crystalline than granular starches and it is, therefore, conceivable that iodine uptake occurs in amorphous portions of the starch granule. In such a case, iodine may complex with a single helical portion of non-crystalline amylose or a linear branch of amylopectin, occupying the cavity inside a V-type helix as had been originally proposed[7,8]. It seems that this point could be resolved by further X-ray diffraction study of iodine–amylose complexes.

The interesting question still remains: why do different plants synthesize starch in different polymorphic forms? Because the B-starch contains considerably more water than A-starch, is there a difference in the amount of water present in the

environments when the two types of starch are synthesized? The latter circumstance may be plausible, because when a solution of any starch (or amylose) is allowed to gel at room temperature, the gel crystallizes and exhibits the X-ray pattern of B-starch.

ACKNOWLEDGMENT

This work was supported by National Science Foundation grant No. CHE7501560.

REFERENCES

1 H. C. H. Wu and A. Sarko, *Carbohydr. Res.*, 54 (1977) C3–C6.
2 H. C. H. Wu and A. Sarko, *Carbohydr. Res.*, 61 (1978) 7–25.
3 J. Blackwell, A. Sarko, and R. H. Marchessault, *J. Mol. Biol.*, 42 (1969) 379–383.
4 R. E. Franklin and R. G. Gosling, *Acta Crystallogr.*, 6 (1953) 678–685.
5 P. Zugenmaier and A. Sarko, *Biopolymers*, 15 (1976) 2121–2136.
6 S. Arnott and W. E. Scott, *J. Chem. Soc. Perkin Trans. 2*, (1972) 324–335.
7 R. E. Rundle, *J. Am. Chem. Soc.*, 69 (1947) 1769–1772.
8 B. Zaslow and R. L. Miller, *J. Am. Chem. Soc.*, 83 (1961) 4378–4381.